Multiple $Bi_2Sr_{2-x}Ba_xCuO_y$ microstructures and the effect of element doping (Ba,La,Pb) on the 2:2:0:1 phase

Mao Zhiqiang, Fan Chenggao, Shi Lei, Yao Zhen, Yang Li, and Wang Yu
Structure Research Laboratory, University of Science and Technology of China, Academia Sinica, Hefei, Anhui 230026, People's Republic of China

Zhang Yuheng
Structure Research Laboratory, University of Science and Technology of China, Academia Sinica, Hefei, Anhui 230026, People's Republic of China
and Chinese Center of Advanced Science and Technology (World Laboratory), P.O. Box 8730, Beijing, People's Republic of China
(Received 27 May 1992; revised manuscript received 20 January 1993)

The microstructure of $Bi_2Sr_{2-x}Ba_xCuO_y$ ($0 \le x \le 0.5$) was characterized by transmission-electron microscopy and x-ray diffraction. Electron-diffraction analyses reveal that in the Bi-Sr-Cu-O system there also exists a $c = 12.5$ Å insulating phase with commensurate superstructure with the exception of the $c = 24$ Å 2:2:0:1 phase. However, with the partial substitution of Ba for Sr in this material, the $c \sim 24$ Å 2:2:0:1 single phase is obtained, but Ba intercalation reduces the wavelength of modulation of the 2:2:0:1 phase along the b and c directions. Measurement of the superconductivity of the $Bi_2Sr_{2-x}Ba_xCuO_y$ samples shows that the appropriate substitution of Ba for Sr ($x \le 0.2$) can raise the T_c of the 2:2:0:1 phase. T_c reaches 20 K for the $x = 0.2$ sample, however, with excessive Ba substitution ($x \ge 0.2$) the metal-to-insulator transition for the 2:2:0:1 phase occurs and the superconductivity of the 2:2:0:1 phase disappears as x exceeds 0.3. In addition, the influence of La and Pb doping on the modulation structure of the 2:2:0:1 phase is also investigated in this article. We discuss the modulation structures of the three substituted systems and the origin of the incommensurate-modulation structure of the Bi-Sr-Cu-O system.

I. INTRODUCTION

In Bi-oxide superconductors the following four superconducting phases have been found with chemical compositions $Bi_2Sr_2Ca_{n-1}Cu_nO_{2n+\delta}$ ($n = 1,2,3,4$).[1,2] The T_c of the $n = 1$, 2, and 3 phases is ~ 20, 85, and 110 K, respectively. The $n = 4$ phase has only been observed in the study of convergent-beam electron diffraction and the bulk superconductor with the $n = 4$ phase has never been observed, so the T_c of the $n = 4$ phase has not been determined. Even though the $n = 1$ phase has low T_c, in recent years, in the field of the fundamental study of Bi-based materials, the focus of attention turns to the $n = 1$ 2:2:0:1 phase. This is due to the fact that this 2:2:0:1 superconducting phase exhibits a much wider temperature region where the normal state exists, which allows one to measure normal-state transport properties to lower temperatures than in other high-T_c materials. Understanding of the nature of the normal state is necessary for the study of the mechanism for high-T_c superconductivity.

However, it is well known that the preparation of 2:2:0:1 single-phase samples in the Bi-Sr-Cu-O system is difficult because of the presence of other insulating phases, and most of the early reports of superconductivity in this material have been on multiphase ceramics.[3–7] Chakoumakos *et al.*[8] and Fleming *et al.*[9] thought that the synthesis was complicated by an insulating phase with a composition that is very close to the stoichiometric composition $Bi_2Sr_2CuO_y$. Fujiki *et al.*[10] suggested that there are at least two other insulating compounds in the Bi-Sr-Cu-O system and that these nonsuperconducting phases have structures which are different but closely related to that of the superconducting phase. In Ref. 11, Matsui *et al.* further determined the microstructural features of these nonsuperconducting Bi-Sr-Cu-O compounds by means of electron-diffraction analyses, which explicitly indicate that in the Bi-Sr-Cu-O system there exist three nonsuperconducting phases (B-D) which have long-period structures closely related to that of the superconducting phase A, $Bi_2Sr_2CuO_y$, and in phase B the long periodicity is caused by the displacements of the $(BiO)_2$ planes along the c axis, while in both phases C and D, it is due to the formations of thin vertical planes of different local structures and compositions. All of these above-mentioned results suggest that the structure of the superconducting 2:2:0:1 phase has an instability at high temperature, so a sample with a single phase is difficult to obtain. In substituted Bi-Sr-Cu-O systems, i.e., $Bi_{2+x}Sr_{2-x}CuO_y$,[12] $Bi_2Sr_{2-x}La_xCuO_y$,[13–16] and $Bi_{2-x}Pb_xSr_2CuO_y$,[17,18] it was found that the ideal 2:2:0:1 single phase can be easily acquired. This suggests that the substitution can stabilize the 2:2:0:1 structures. Yet, the type of element substituted has serious effects on the superconductivity of the 2:2:0:1 phase, as is reported in Refs. 12–18. For the $Bi_{2+x}Sr_{2-x}CuO_y$ and $Bi_2Sr_{2-x}La_xCuO_y$ systems, the emergence of superconductivity of the 2:2:0:1 phase depends critically on the minimum Sr content, and a metal-insulator transition also occurs with the variation of Sr composition. According to all the above reports, one can see that the

phase diagram for 2:2:0:1 ceramic samples is complex, and the structure of the crystal grown under specific conditions cannot be easily asserted. In that way, it is quite evident that further investigation into the formation of the 2:2:0:1 phase, as well as its microstructural characteristic features, is of great significance. Hence, we synthesized three series of doped 2:2:0:1 ceramic sample, i.e., $Bi_2Sr_{2-x}Ba_xCuO_y$, $Bi_{2.1}Sr_{1.9-x}La_xCuO_y$, and $Bi_{2-x}Pb_xSr_2CuO_y$, and studied, with emphasis on the synthesis, modulation structure, and superconductivity of the Ba-doped system. Meanwhile by means of the comparison of the modulation structure of the Ba-doped 2:2:0:1 phase with that of La- and Pb-doped 2:2:0:1 phases, a speculative discussion is made for the origin of incommensurate-modulation structure of Bi-system materials.

II. EXPERIMENTAL METHODS

Samples were prepared by the conventional solid-state reaction method. Powders of Bi_2O_3, PbO, $SrCO_3$, $BaCO_3$, La_2O_3, and CuO were mixed with nominal compositions of $Bi_2Sr_{2-x}Ba_xCuO_y$ ($x=0$, 0.1, 0.2, 0.3, 0.4, and 0.5), $Bi_{2.1}Sr_{1.9-x}La_xCuO_y$ ($x=0.1$, 0.2, 0.3, 0.4, 0.6, and 1.0), and $Bi_{2-x}Pb_xSr_2CuO_y$ ($x=0.05$, 0.1, 0.2, 0.3, and 0.6), respectively, then preheated in air at 820 °C. In order to ensure the complete reaction of the reactant oxides, the products were then reground and reheated at 830 °C. Preheating took place for about 32–40 h. Then the powders were pressed into pellets, sintered in air in the temperature range of 860–910 °C for 70–140 h (higher temperature is required for Ba- and La-doped samples, and lower temperature for Pb-doped samples), and finally quenched in air.

X-ray-diffraction (XRD) analysis was carried out with Ligaku D/max- γA diffractometer using monochromatic high-intensity Cu-$K\alpha$ radiation at room temperature. Electron-diffraction (ED) patterns were obtained using a H-800 transmission-electron microscopy. The specimens for TEM observation were prepared by the ion milling method. Resistivity was measured by the standard four-probe method.

III. EXPERIMENTAL RESULTS

A. XRD analyses for the samples $Bi_2Sr_{2-x}Ba_xCuO_y$ ($0 \le X \le 0.5$), $Bi_{2.1}Sr_{1.9-x}La_xCuO_y$ ($0.1 \le X \le 1.0$), and $Bi_{2-x}Pb_xSr_2CuO_y$ ($0.05 \le X \le 0.6$)

Figure 1 shows the XRD patterns of the samples $Bi_2Sr_{2-x}Ba_xCuO_y$ ($x=0$, 0.1, 0.2, 0.3, 0.4, and 0.5). From these XRD patterns, first it can be noted that in the case of $x=0.0$, the (001) diffraction peaks split into doublets, while other characteristic peaks are obviously broadened. This implies that in this sample there exists structural inhomogeneity, i.e., other nonsuperconducting phases as reported in Refs. 10 and 11 probably appear. Secondly, for the Ba-doped samples, the XRD patterns show that the ideal pure 2:2:0:1 single phases are obtained. This result indicates that the intercalation of Ba into the Bi-Sr-CuO system plays an important role in synthesizing the 2:2:0:1 single phase. On the other hand, Fig. 1 reflects the fact that the position of the typical diffraction peaks of 2:2:0:1 phase changes successively with the increase of Ba content and suggests that the unit-cell parameters of the Ba-doped 2:2:0:1 phase vary correspondingly, as shown in Table I (obtained from a least-squares refinement). The data given in Table I show that the length of the c axis of the 2:2:0:1 phase decreases with the increase of Ba content, while the a and b axes and the orthorhombicity of the 2:2:0:1 phase increase accordingly.

The XRD analyses of $Bi_{2.1}Sr_{1.9-x}La_xCuO_y$ and $Bi_{2-x}Pb_xSr_2CuO_y$ show that the La substitution for Sr and Pb for Bi are similarly beneficial to the synthesis of 2:2:0:1 single phase, i.e., for the case of $x>0$ in the two systems, the ideal 2:2:0:1 single phases are also obtained.

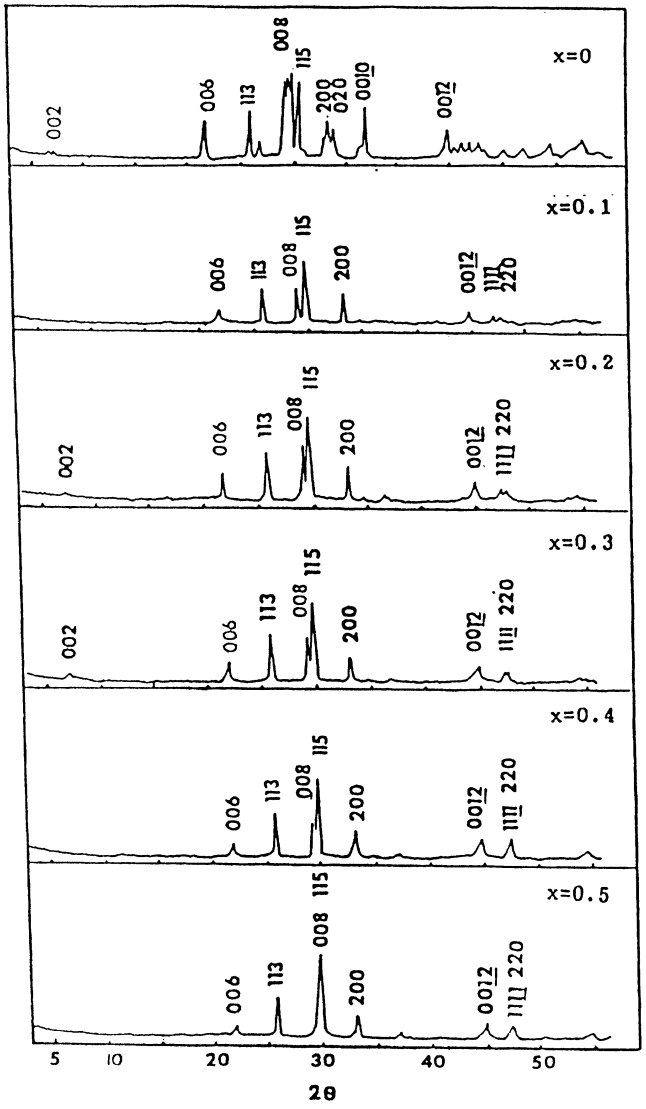

FIG. 1. The powder x-ray-diffraction patterns of $Bi_2Sr_{2-x}Ba_xCuO_y$ samples ($x=0$, 0.1, 0.2, 0.3, 0.4, and 0.5).

TABLE I. Structural parameters of the $Bi_2Sr_{2-x}Ba_xCuO_y$ systems.

Ba content x	a (Å)	b (Å)	c (Å)	q_b/b
0.1	5.364	5.364	24.535	4.86
0.2	5.369	5.367	24.481	4.32
0.3	5.384	5.378	24.412	4.30
0.4	5.390	5.395	24.334	4.22
0.5	5.416	5.439	24.172	4.14

TABLE III. Structural parameters of the $Bi_{2-x}Pb_xSr_2CuO_y$ systems.

Pb content x	a (Å)	b (Å)	c (Å)
0.05	5.373	5.370	24.641
0.1	5.350	5.343	24.561
0.2	5.383	5.306	24.540
0.3	5.376	5.276	24.533
0.6	5.378	5.250	24.456

The variation of structural parameters of the 2:2:0:1 phase induced by the two different substitutions is summarized in Tables II and III, respectively, which show that the orthorhombicity of the 2:2:0:1 phase also increases with La substitution for Sr or Pb substitution for Bi, as is indicated in Refs. 13–18. It is worthwhile noticing that the behavior of the variation of the b axis for the Ba- and La-doped systems is in agreement but opposite to that of the Pb-doped system.

B. ED analyses for the samples $Bi_2Sr_{2-x}Ba_xCuO_y$ ($0 \le X \le 0.5$), $Bi_{2.1}Sr_{1.9-x}La_xCuO_y$ ($0.1 \le X \le 1.0$), and $Bi_{2-x}Pb_xSr_2CuO_y$ ($0.05 \le X \le 0.6$)

1. *Multiple 2:2:0:1 microstructures in the $Bi_2Sr_2CuO_y$ sample*

Figures 2(a)–2(c) show the [100]-zone-axis ED patterns for the undoped sample. The ED pattern of Fig. 2(a) appears in most of the observed grains, while those Figs. 2(b) and 2(c) are only exhibited in a few crystal grains. The sequences of satellite spots in Fig. 2(a) reflect the monoclinic incommensurate-modulation structure of the $c=24$ Å 2:2:0:1 phase, as is reported in Refs. 4, 10, 19, and 20. The study with a high-resolution electron microscope has revealed that this kind of incommensurate modulation is due to the periodic arrangement of Bi-concentrated and deficient bands in the BiO double layers. However, the ED pattern shown in Fig. 2(c) exhibits a similar feature with the phase B reported in Ref. 11, namely it reflects a type of monoclinic modulation structure with the corresponding c parameter of 12.5 Å. The main difference between the two phases is that the modulation structure reflected in Fig. 2(c) is commensurate but is incommensurate for phase B in Ref. 11. From high-resolution images, the authors of Ref. 11 found that the superstructure of phase B is caused by periodic arrangement of the BiO layers, which are interrupted at every 2.0 nm along the b axis and displaced by xc, where x is nearly 0.2. Therefore, we can assert that in the $Bi_2Sr_2CuO_y$ sample two phases exist, one is the $c=24$ Å 2:2:0:1 phase with incommensurate-modulation structure and the other is the $c=12.5$ Å nonsuperconducting phase with commensurate long-period superstructure. So the behavior of the doublet-split XRD pattern of the $Bi_2Sr_2CuO_y$ sample can be understood quite well. Moreover, it should be mentioned that the two kinds of ED patterns of Figs. 2(a) and 2(c) can appear in different regions of a small fragment, and it means that the intergrowth occurs between the two phases.

TABLE II. Structural parameters of the $Bi_{2.1}Sr_{1.9-x}La_xCuO_y$ systems.

La content x	a (Å)	b (Å)	c (Å)	q_b/b
0.1	5.368	5.365	24.57	4.90
0.2	5.374	5.376	24.515	4.33
0.3	5.407	5.419	24.519	4.22
0.4	5.389	5.395	24.249	4.15
0.6	5.415	5.448	24.175	4.09
1.0	5.451	5.504	24.115	4.00

For the ED pattern of Fig. 2(b), it is clearly seen that it exhibits a very peculiar feature, i.e., all the satellite spots in this pattern are symmetric about the c^* or b^* axis. This type of b^*-c^*- plane electron-diffraction pattern has been reported by Van Tandeloo *et al.*,[21] who suggested that it results from the two variants of structural modulation which are related by a symmetry plane along (001), and a mirror plane is located at the bismuth oxide layer.

2. *Effect of Ba doping on the modulated structure of the 2:2:0:1 phase*

From the analyses of the [001]-zone ED patterns of samples $Bi_2Sr_{2-x}Ba_xCuO_y$ ($x=0.1$, 0.2, 0.3, 0.4, and 0.5), the b component of modulation vector, q_b, for each sample can be determined, as shown in Table I. From Table I, it can be seen that the value of q_b/b decreases from 4.86 to 4.14 with the Ba content x increasing from 0.1 to 0.5. Figures 3(a1), 3(a2), 3(b1), 3(b2), 3(c1), and 3(c2) show two series of [100]-zone ED patterns observed in the sample of $x=0.2$, 0.3, and 0.5. Clearly, the ED patterns shown in Figs. 3(a1), 3(b1), and 3(c1) belong to the same series, the satellite sequences of which reflect the conventional monoclinic incommensurate-modulation structure of the Bi-2:2:0:1 phase. According to the three ED patterns, the corresponding modulation vector in b^*-c^* plane, $q^*=\beta b^*+\gamma c^*$, can be identified as

$$q_1^*=0.23b^*+0.51c^* \quad (x=0.2),$$

$$q_2^*=0.23b^*-0.76c^* \quad (x=0.3),$$

$$q_3^*=0.25b^*+0.8c^* \quad (x=0.5),$$

respectively. [The estimated error for the modulation wave vector: $\Delta\beta$ (or $\Delta\gamma$) ≤ 0.005.] As a result, it can be noticed that the c^* component of the modulation vector increases with an increase of Ba composition. Figures 3(a2), 3(b2), and 3(c2) exhibit the other series of [100]-

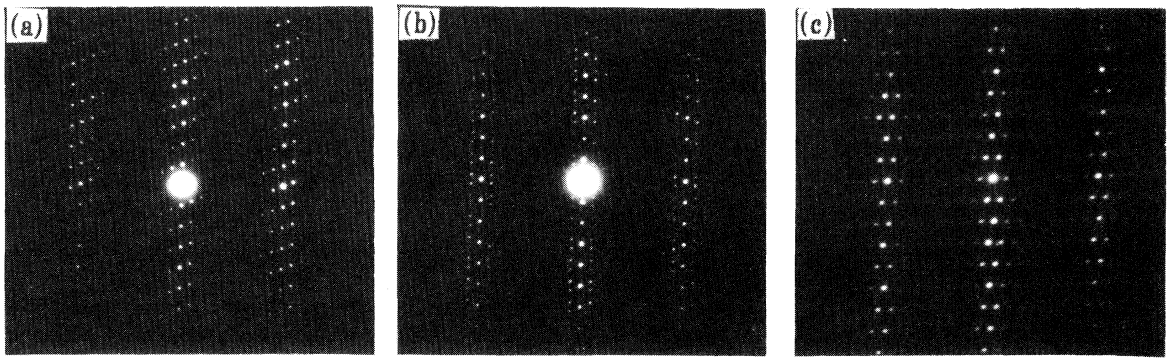

FIG. 2. The three kinds of different ED patterns along the [100]-zone axis of the sample $Bi_2Sr_2CuO_y$.

zone ED patterns observed in the three samples, which all possess the same features as that shown in Fig. 2(b), that is, all satellite diffraction spots are symmetric about the b^* or c^* axis. The noteworthy point is that the three ED patterns shown in Figs. 3(a2), 3(b2), and 3(c2) exhibit different features, i.e., the distance between two adjacent satellite spots of the first order along the c^* direction (denoted by l below) decreases with an increase of Ba content. In fact, the variation of l with Ba content x results from the change of modulation vector (i.e., the increase of c^* component). This behavior can be interpreted from the schematic diagram of Figs. 4(a)–4(c). Figures

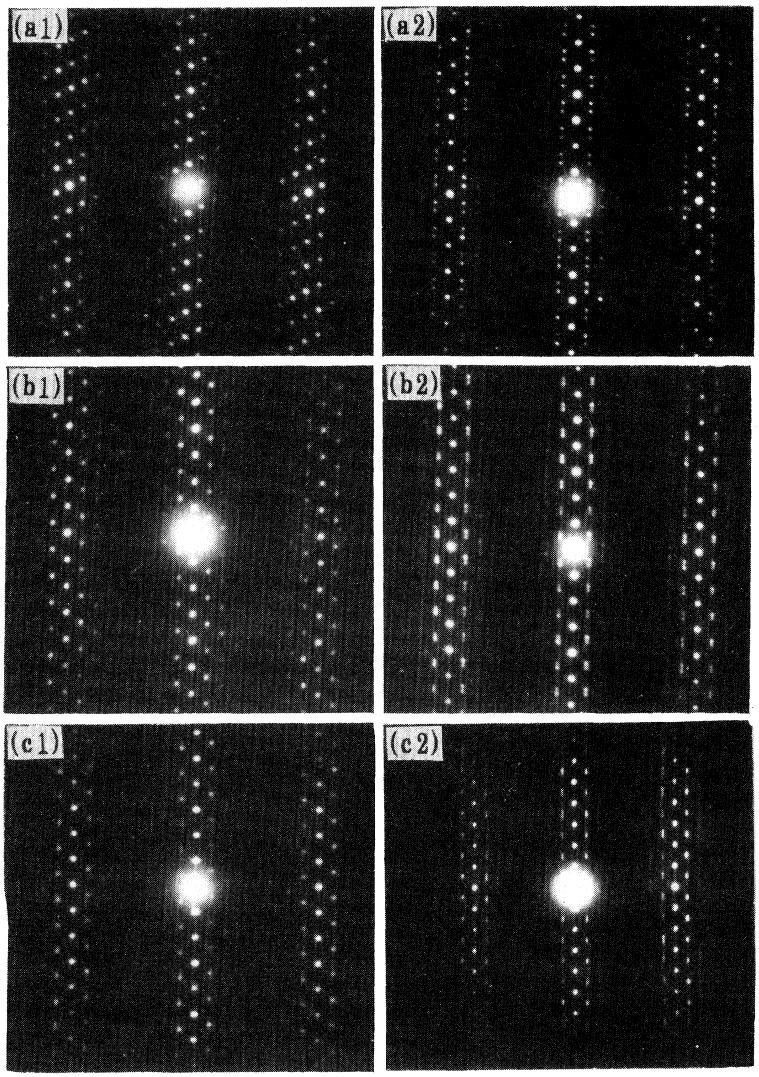

FIG. 3. (a1)-(a2), (b1)-(b2), and (c1)-(c2) are the two series of [100]-zone ED patterns observed in the samples $Bi_2Sr_{1.3}Ba_{0.2}CuO_y$, $Bi_2Sr_{1.7}Ba_{0.3}CuO_y$, and $Bi_2Sr_{1.5}Ba_{0.5}CuO_y$, respectively.

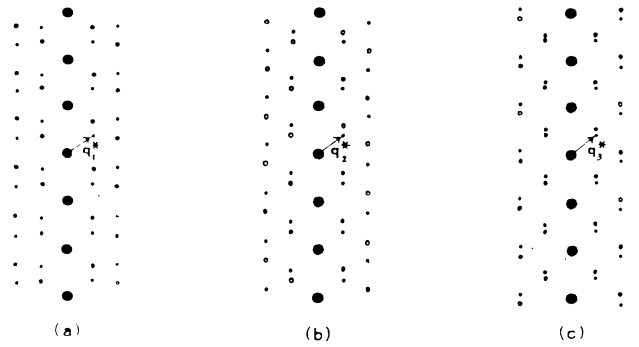

FIG. 4. Schematic diagram of [100]-zone coplanar ED patterns corresponding to the three different modulation wave vectors, i.e., $q_1=\beta_1 b^*+\gamma_1 c^*$, $q_2=\beta_2 b^*+\gamma_2 c^*$, $q_3=\beta_3 b^*+\gamma_3 c^*$, $\beta_1=\beta_2=\beta_3$, and $\gamma_1<\gamma_2<\gamma_3$.

4(a)–4(c) give the three [100]-zone coplanar diffraction schematic diagrams with different modulation vectors ($\beta_1=\beta_2=\beta_3$, $\gamma_1<\gamma_2<\gamma_3$). It shows that the increase of γ component of the modulation vector really result in the reduction of the l value. In other words, the variation of l shown in Figs. 3(a2), 3(b2), and 3(c2) directly reflect the change of modulation vector of the 2:2:0:1 phase induced by Ba doping.

In addition, it should be pointed out that for $x=0.5$ sample, the satellite spots of [100]-zone ED patterns elongate along the c^* direction feebly, as shown in Figs. 3(c1) and 3(c2). This implies that the small distortion happens for the periodic arrangement of Bi-concentrated bands. Figures 5(a)–5(c) exhibit the [010]-zone ED patterns of the three different samples ($x=0.2$, 0.3, and 0.5), in which no difference among the three samples can be observed. It is known that the presence of weak reflection $(101)+n(002)$ is mainly due to the displacement of Bi atoms from special positions of the orthorhombic *Fmmm* space group in the average structure.[22] So, based on this argument, it can be postulated that the distortion, which happens in double BiO layers, is not serious.

3. *Effect of La and Pb doping on the modulated structure of the 2:2:0:1 phase*

From the structural parameters of $Bi_{2.1}Sr_{1.9-x}La_xCuO_y$ as shown in Table II, it can be seen that the value of q_b of the La-doped 2:2:0:1 phase decreases with an increase of La composition. On the other hand, the modulation vector containing b^* and c^* components for the different La-doped 2:2:0:1 phases is also obtained from the corresponding [100]-zone ED patterns shown in Figs. 6(a1)–6(a3). These wave vectors can be expressed as follows:

$$q_1^*=0.23b^*+0.64c^* \quad (x=0.2)\,,$$

$$q_2^*=0.24b^*+0.94c^* \quad (x=0.6)\,,$$

$$q_3^*=0.25b^*+1.0c^* \quad (x=1.0)\,,$$

thus it is found that similar to the Ba-doped 2:2:0:1 phase, the c^* component of the modulation vector of the La-doped 2:2:0:1 phase also increases with increasing La dopant. For the [100]-zone ED patterns shown in Figs. 6(a1)–6(a3), another two important features are as follows: On one hand, for higher La-content samples ($x=0.6$, 1.0) all the satellite spots as shown in Figs. 6(a2) and 6(a3) also elongate slightly along c^* axis, increasingly changing from circle spots to elliptical, however, the $n(002)$ main reflection nearly remains intact; on the other hand, with increasing La content the modulation along b direction transforms from incommensurate (corresponding to the case of $x=0.2$, 0.4, and 0.6) to commensurate (corresponding to the case of $x=1.0$).

The ED patterns along the pole of [100] of the samples $Bi_{2-x}Pb_xSr_2CuO_y$ ($x=0$, 0.05, 0.2, 0.3, and 0.6) are shown in Figs. 7(a)–7(e). Figure 8 gives the corresponding schematic representation of these ED patterns. For the [100]-zone ED patterns of the $x=0$ samples shown in Fig. 7(a), as described in the preceding part, its satellite sequences only reflect the monoclinic modulation structure. However, for the $x=0.05$ sample, in its [100]-zone ED pattern, another kind of satellite reflection spot appears: it reveals that two types of modulation coexist in this sample (i.e., the monoclinic modulation and orthorhombic modulation), while for $x=0.2$, 0.3 samples the

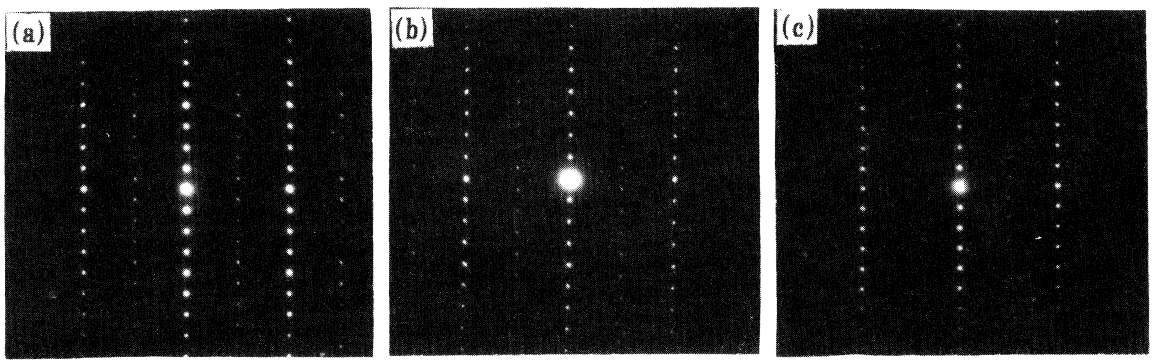

FIG. 5. The [010]-zone ED patterns observed in the samples $Bi_2Sr_{2-x}Ba_xCuO_y$; (a) $x=0.2$; (b) $x=0.3$; (c) $x=0.5$.

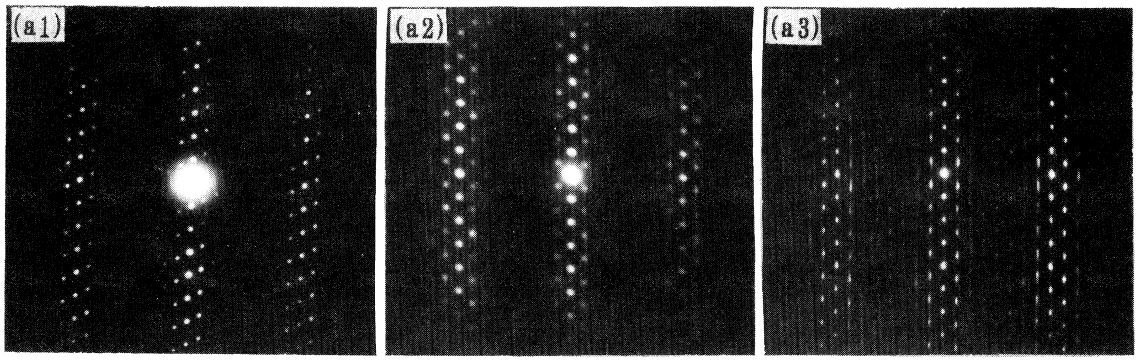

FIG. 6. The ED patterns along the [100]-zone axis of the samples $Bi_{2.1}Sr_{1.9-x}La_xCuO_y$; (a1) $x=0.2$; (a2) $x=0.6$; (a3) $x=1.0$.

satellite reflections corresponding to monoclinic modulation disappear completely and merely the orthorhombic modulation induced by Pb doping exists, simultaneously accompanied with the increase of the modulation wavelength. With the further increase of Pb content ($x=0.6$), all the modulation modes disappear. This type of modulation structure transition caused by Pb doping in the 2:2:0:1 phase is consistent with the result reported in Ref. 18.

IV. SUPERCONDUCTIVITY OF THE $Bi_2Sr_{2-x}Ba_xCuO_y$ ($0 \le X \le 0.5$) SAMPLES

The temperature dependence of resistivity of samples $Bi_2Sr_{2-x}Ba_xCuO_y$ ($x=0$, 0.1, 0.2, 0.3, 0.4, and 0.5) is shown in Fig. 9(a). For these samples with different Ba content, the above XRD and ED analyses have revealed that they all exhibit ideal 2:2:0:1 single phase except for the case of $x=0$. But the result of resistivity measurement of these samples given by Fig. 9(a) shows that great differences among their electrical properties appears. When the Ba content x increases from 0 to 0.2, the corresponding initial superconducting transition temperature, T_c^{onset}, increases from 10 to 20 K, but with $x=0.3$, the T_c^{onset} decreases to 9 K again, and with the further increase of Ba content x ($x=0.4$, 0.5), the sample becomes a semiconductor. The relation between T_c^{onset} and the Ba content x of the $Bi_2Sr_{2-x}Ba_xCuO_y$ system is depicted in Fig. 9(b). Moreover, it is also found that the suitable Ba doping ($x<0.2$) can decrease the magnitude of normal-

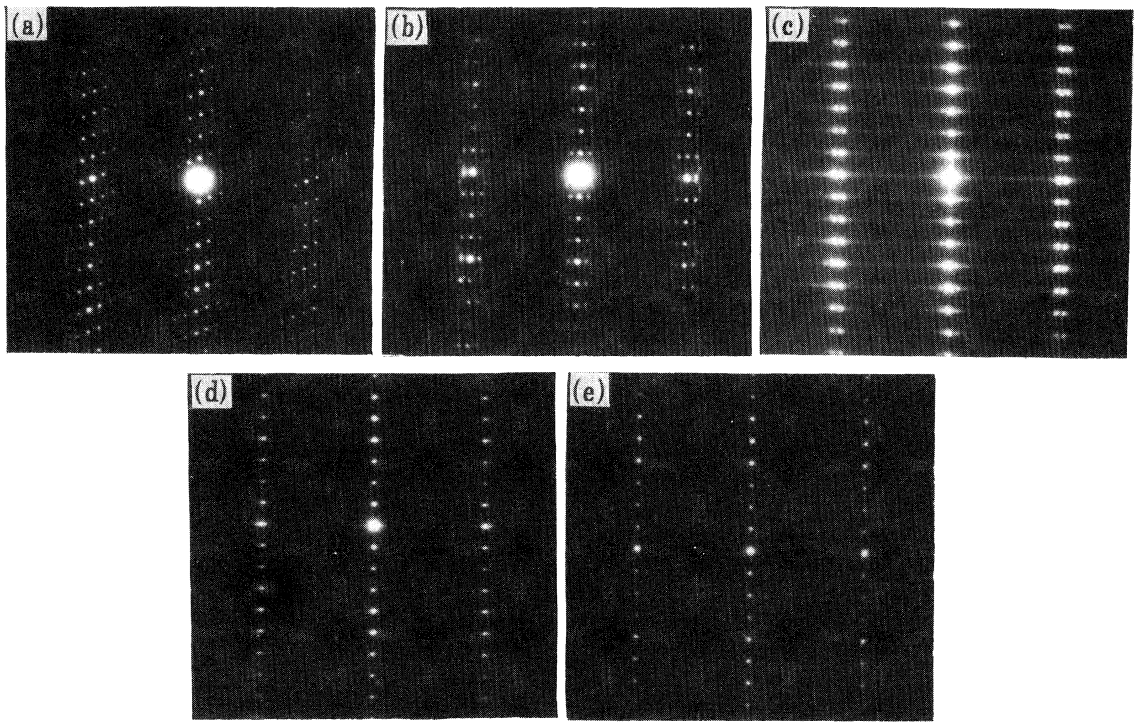

FIG. 7. The ED patterns along the [100]-zone axis of the samples $Bi_{2-x}Pb_xSr_2CuO_y$; (a) $x=0$; (b) $x=0.05$; (c) $x=0.2$; (d) $x=0.3$; (e) $x=0.6$.

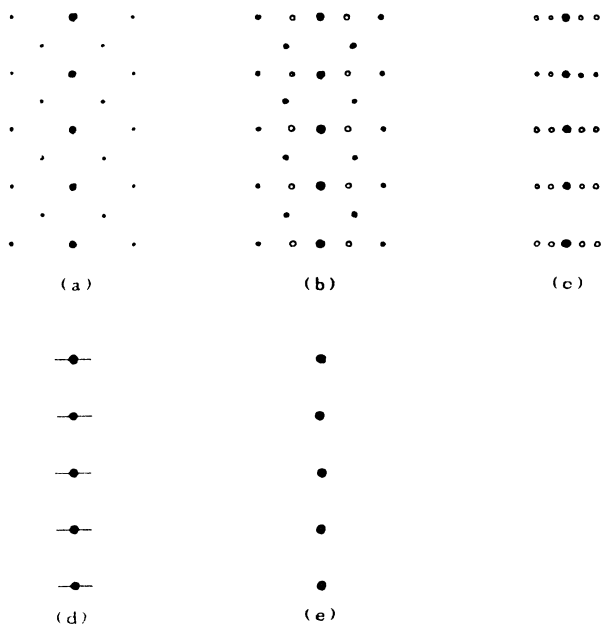

FIG. 8. The schematic representation of the ED patterns of Figs. 7(a)–7(e); (a) $x=0$; (b) $x=0.05$; (c) $x=0.2$; (d) $x=0.3$; (e) $x=0.6$. The satellite reflection spots (marked with .) correspond to monoclinic modulation and the other series (marked with ∘) correspond to orthorhombic modulation.

state resistivity, which is increased rapidly, however, by excessive Ba doping ($x>0.2$). Consequently, it can be concluded that the appropriate amount of Ba substitution for Sr can improve the superconductivity of 2:2:0:1 phase but excessive substitution leads to the emergence of metal-to-insulator transition.

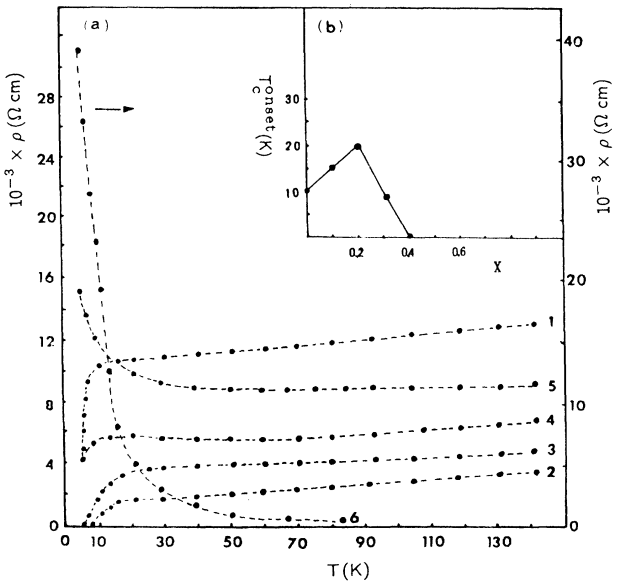

FIG. 9. (a) The temperature dependence of resistivity of the samples $Bi_2Sr_{2-x}Ba_xCuO_y$; 1, $x=0$; 2, $x=0.1$; 3, $x=0.2$; 4, $x=0.3$; 5, $x=0.4$; 6, $x=0.5$. (b) The relationship between T_c^{onset} and Ba content x.

V. DISCUSSION

A. The origin of incommensurate-modulation structure in the Bi-2:2:0:1 system

It has already been pointed out that the modulation structure of the Bi-based oxide superconductors originates from the periodic arrangement of Bi-concentrated bands in BiO layers. Such an arrangement is caused by the lattice mismatch between BiO layers and perovskite blocks. As to what is the real driving force of the lattice mismatch, several possible models were proposed by Zandbergen and Gay and co-workers,[23–25] mainly including: (1) the extra oxygen model, (2) ordering of Sr vacancies, (3) partial substitution of Bi by Cu, and (4) changes in the orientation of Bi lone pairs. In these models, the first one (i.e., the extra oxygen model) is the most well known. But there also exist some serious weaknesses associated with this model, for example, when one performs the ED analyses at high temperature for the superconducting phase of Bi-system compound, it is discovered that as the temperature goes up to 1000 K, the intensity, sharpness, as well as the distance between reciprocal spots of the superstructure reflection display no observed changes. This implies that the intensity of the superstructure modulation is insensitive to the change of oxygen content. Therefore, some other possible models could not be eliminated.

However, on the basis of the investigation of the modulation structures for the above-mentioned three substituted 2:2:0:1 systems, i.e., $Bi_{2-x}Pb_xSr_2CuO_y$, $Bi_{2.1}Sr_{1.9-x}La_xCuO_y$, and $Bi_2Sr_{2-x}Ba_xCuO_y$, we think that the real driving force which results in superstructure modulation comes from the crystal misfit along b axis between the Bi_2O_3 of the BiO layer and perovskite. The variation of this type of misfit degree along the b axis will directly induce the rearrangement of Bi-concentrated bands of the BiO layer, thus giving rise to the change of the modulation wave vector within BiO layers. In the $Bi_{2-x}Pb_xSr_2CuO_y$ system, it has been revealed that with the substitution of Pb for Bi, the length of the b axis decreases. The reduction of the b axis enhances the fit degree between the BiO layer and the perovskite block, and the arrangement pattern of Bi-concentrated bands is softened. Therefore, with increasing Pb content, the monoclinic modulation disappears gradually, while Pb-type modulation becomes dominant. The latter probably originates from the periodic distribution of Pb atoms in BiO double layers. However, for the La- and Ba-doped systems, due to the larger ion radius of the doped element, La (or Ba), which is suggested to occupy the Sr sites, the a and b parameters of the perovskite block increase, with the latter changing more remarkably than the former, so the misfit degree between the BiO layer and the perovskite block along the b axis strengthens, thus decreasing the periodicity of the Bi-concentrated band; this point agrees well with our experiment results. As a result, we draw this conclusion: The variation of modulation vector induced by element doping in Bi-superconductors originates from the change of the misfit degree between BiO layers and perovskite blocks, and the

misfit degree mainly depends on the size of the perovskite block (primarily the length of the b axis), the larger the b parameter, the lower the crystal-fit degree. The above-mentioned elongation of the satellite reciprocal spots as shown in Figs. 3 and 6 and the modulation transition of incommensurate-to-commensurate observed in the La-doped system all reflect the enhancement of the misfit degree between the BiO layer and the perovskite block induced by element substitution in essence.

Here, it should be pointed out that the lattice misfit model we are discussing essentially does not contradict the above-mentioned model as argued by Zandbergen and co-workers. It is because this type of crystal misfit between the BiO layer and the perovskite block, as we proposed, would probably directly result in inhomogeneous distribution of oxygen atoms in BiO double layers, namely, extra oxygen may emerge in the BiO layer. In addition, Bi vacancies in the BiO layer or Sr vacancies in the SrO layer may also occur in this case, while other atoms may occupy these vacancies, which would probably lead to the modulation of the distribution of occupation.

B. Correlation between microstructure and superconductivity of the 2:2:0:1 phase in the $Bi_2Sr_{2-x}Ba_xCuO_y$ system

In Refs. 26 and 27, Onoda and Sato and Gao *et al.* have already investigated the incommensurate-modulation structure of superconducting Bi-Sr-Cu-O system by means of single-crystal x-ray diffraction, indicating that the modulation wave of the Bi-Sr-Cu-O system causes swelling of each layer, i.e., the displacements of Bi, Sr, and Cu in the chains which run along the c axis. The deviation of the Cu-atom positions caused by the modulation wave in the 2:2:0:1 phase is much larger than that in the 2:2:1:2 phase, which may be one of the origins of the rather low-T_c value of the Bi-Sr-Cu-O compound. Then, in the $Bi_2Sr_{2-x}Ba_xCuO_y$ system, as is well known, the Ba substitution for Sr does not directly induce the change of the number of electrons of the 2:2:0:1 phase such that the variation of superconductivity of the Ba-doped 2:2:0:1 phase can only be attributed to the microstructural distortions, namely the change of modulation structure. In terms of the ideas of Onoda and Sato and Gao *et al.*, it can be considered that the decrease of the modulation period in the b and c direction is certain to lead the Cu displacement to a relative shift, thus resulting in the change of the oxygen configuration of Cu atoms, which is closely related to the superconductivity of the 2:2:0:1 phase. That is to say, the proper substitution of Ba for Sr is favorable to improve the symmetric degree of the CuO_2 layer, and just for this reason the T_c of the 2:2:0:1 phase is raised, while for excessive Ba substitution in the Bi-Sr-CuO system, the symmetric degree of the CuO_2 layer was reduced, so that the metal-insulator transition correspondingly appears.

VI. CONCLUSION

From the analyses of the $Bi_2Sr_{2-x}Ba_xCuO_y$ ($0 \le X \le 0.5$), $Bi_{2.1}Sr_{1.9-x}La_x-CuO_y$ ($0.1 \le X \le 1.0$), and $Bi_{2-x}Pb_xSr_2CuO_y$ ($0.05 \le X \le 0.6$) systems, it is found that in the $Bi_2Sr_2CuO_y$ sample, the presence of the $c = 12.5$ Å nonsuperconducting phase is the major reason why the $c = 24$ Å 2:2:0:1 single phase is difficult to synthesize; then Ba partial substitution for Sr in this material can stabilize the $c = 24$ Å 2:2:0:1 phase, and such a substitution has similar influence on the modulation structure and superconductivity of the 2:2:0:1 phase compared with La substitution. On one hand, the Ba substitution causes the reduction of the modulation period, on the other hand it induces the increase of the T_c of the 2:2:0:1 phase with suitable substitution but the emergence of a metal-to-insulator transition with excessive substitution. By way of comparison of the structural parameters of the three substituted systems, it is revealed that the characteristic of modulation wave vectors in the 2:2:0:1 system are indeed dependent on the size of the b axis. This point supplies an important confirmation for the crystal-misfit model for the origin of the incommensurate-modulation structure of Bi superconductors.

[1]H. Maeda, Y. Tanaka, M. Fukutomi, and T. Asano, Jpn. J. Appl. Phys. **27**, L209 (1988).

[2]S. Losch, H. Budin, O. Eibl, M. Hartmann, T. Rentschler, M. Rygula, S. Kemmler-Sack, and R. P. Huebener, Physica C **177**, 271 (1991).

[3]H. Sawa, H. Fujiki, K. Tomimoto, and J. Akimitsu, Jpn. J. Appl. Phys. **27**, L830 (1988).

[4]J. Akimitsu, A. Yamazaki, H. Sawa, and H. Fujiki, Jpn. J. Appl. Phys. **26**, L2080 (1987).

[5]Y. Ikeda, H. Ito, S. Shimomura, Y. Oue, K. Inaba, Z. Hiroi, and M. Takano, Physica C **159**, 93 (1989).

[6]M. Onoda, M. Sera, K. Fukuda, S. Kondoh, M. Sato, T. Den, H. Sawa, and J. Akimitsu, Solid State Commun. **66**, 189 (1988).

[7]T. Ishida and T. Sakuma, Physica C **167**, 258 (1990).

[8]B. C. Chakoumakos, P. S. Ebey, B. C. Sales, and E. Sonder, J. Mater. Res. **4**, 767 (1990).

[9]R. M. Fleming, S. A. Sunshine, L. F. Schneemeyer, R. B. Van Dover, R. J. Cava, P. M. Marsh, J. V. Waszczak, S. H. Glarum, and S. M. Zahurak, Physica C **173**, 37 (1991).

[10]H. Fujiki, M. Sano, K. Tomimoto, H. Sawa, J. Akimitsu, and N. Kitamura, Jpn. J. Appl. Phys. **27**, L1044 (1988).

[11]Y. Matsui, S. Takawa, H. Nozaki, and A. Umezono, Jpn. J. Appl. Phys. **28**, L602 (1989).

[12]G. Xiao, M. Z. Cieplak, and C. L. Chien, Phys. Rev. B **38**, 11 824 (1988).

[13]W. A Groen, D. M. de Leeuw, and G. M. Stallman, Solid State Commun. **72**, 697 (1989).

[14]A. Maeda, M. Hase, I. Tsukada, K. Noda, S. Takebayashi, and K. Uchinokura, Phys. Rev. B **41**, 6418 (1990).

[15]W. A. Groen and H. W. Zandbergen, Solid State Commun. **68**, 527 (1988).

[16]W. Bauhofer, H. Mattausch, R. K. Kremer, P. Murugaraj, and A. Simon, Phys. Rev. B **38**, 7244 (1989).

[17]A. Maeda, Y. Kato, T. Shibauchi, Y. Nakajima, H. Watanabe, and K. Uchinokura, Jpn. J. Appl. Phys. **28**, L1549 (1989).
[18]Y. Matsui, A. Maeda, K. Uchinokura, and S. Takekawa, Jpn. J. Appl. Phys. **29**, 273 (1990).
[19]Y. Matsui, S. Takekawa, S. Horiuchi, and A. Umezono, Jpn. J. Appl. Phys. **27**, L1873 (1988).
[20]C. Michel, M. Hervieu, M. M. Borel, A. Grandin, F. Deslandes, J. Provost, and B. Raveau, Z. Phys. B **68**, 421 (1987).
[21]G. Van Tendeloo, H. W. Zandbergen, J. Van Landuyt, and S. Amelinckx, Appl. Phys. A **46**, 153 (1988).
[22]O. Eibl, Physica C **168**, 215 (1990).
[23]H. W. Zandbergen, W. A. Groen, F. C. Mijhoff, G. Tendeloo, and S. Amelichx, Physica C **168**, 325 (1988).
[24]P. L. Gay and P. Day, Physica C **152**, 335 (1988).
[25]H. W. Zandbergen, W. A. Groen, A. Smit, and G. Van Tendeloo, Physica C **168**, 426 (1990).
[26]M. Onoda and M. Sato, Solid State Commun. **67**, 799 (1988).
[27]Y. Gao, P. Lee, J. Ye, P. Bush, V. Petricek, and P. Coppens, Physica C **160**, 431 (1989).

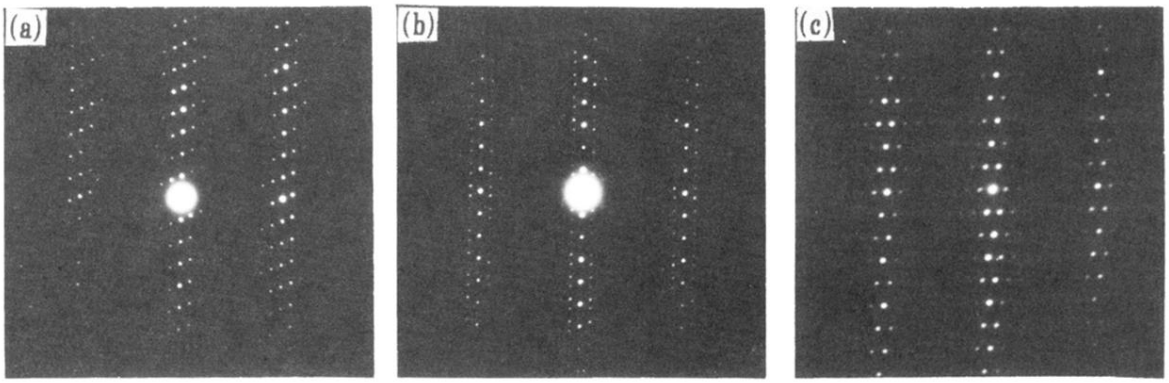

FIG. 2. The three kinds of different ED patterns along the [100]-zone axis of the sample $Bi_2Sr_2CuO_y$.

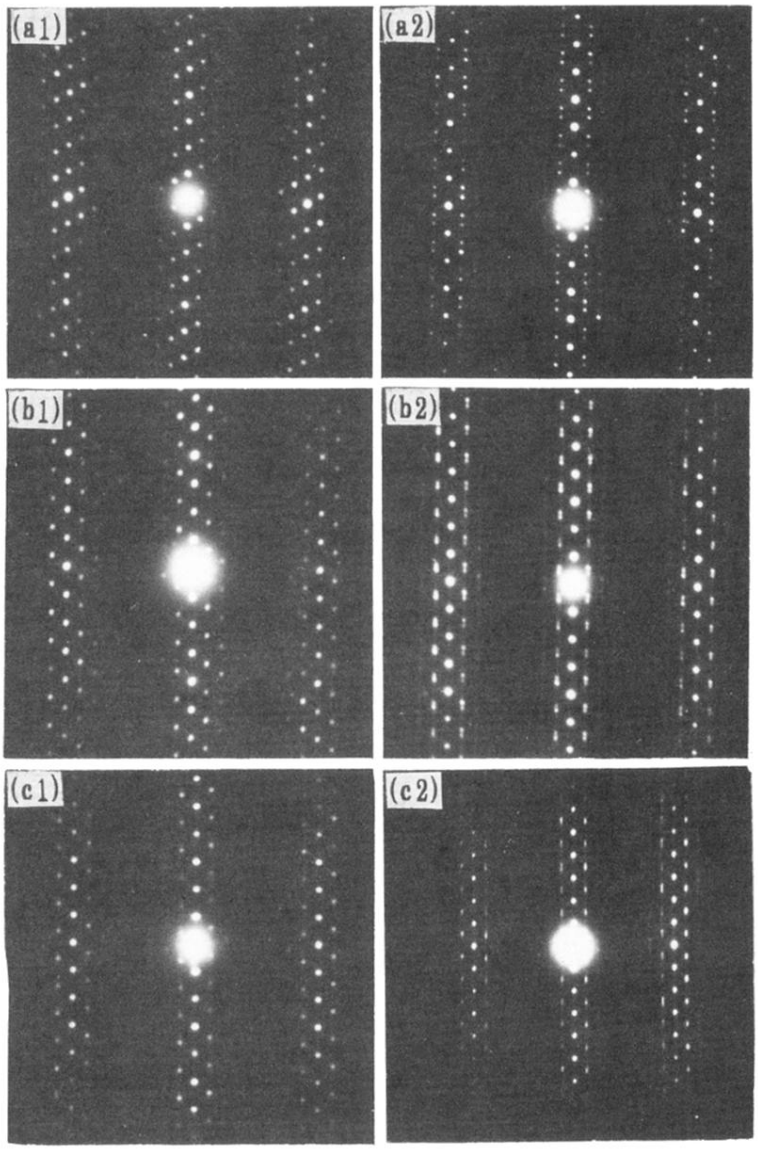

FIG. 3. (a1)-(a2), (b1)-(b2), and (c1)-(c2) are the two series of [100]-zone ED patterns observed in the samples $Bi_2Sr_{1.3}Ba_{0.2}CuO_y$, $Bi_2Sr_{1.7}Ba_{0.3}CuO_y$, and $Bi_2Sr_{1.5}Ba_{0.5}CuO_y$, respectively.

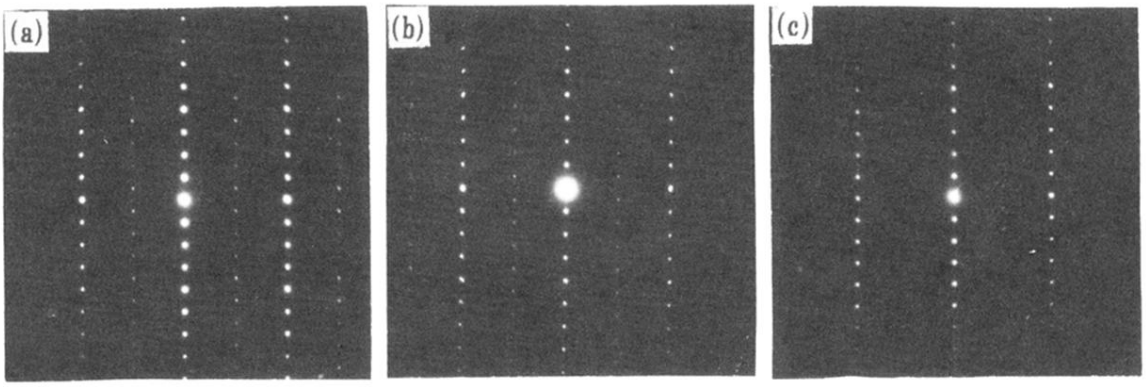

FIG. 5. The [010]-zone ED patterns observed in the samples $Bi_2Sr_{2-x}Ba_xCuO_y$; (a) $x=0.2$; (b) $x=0.3$; (c) $x=0.5$.

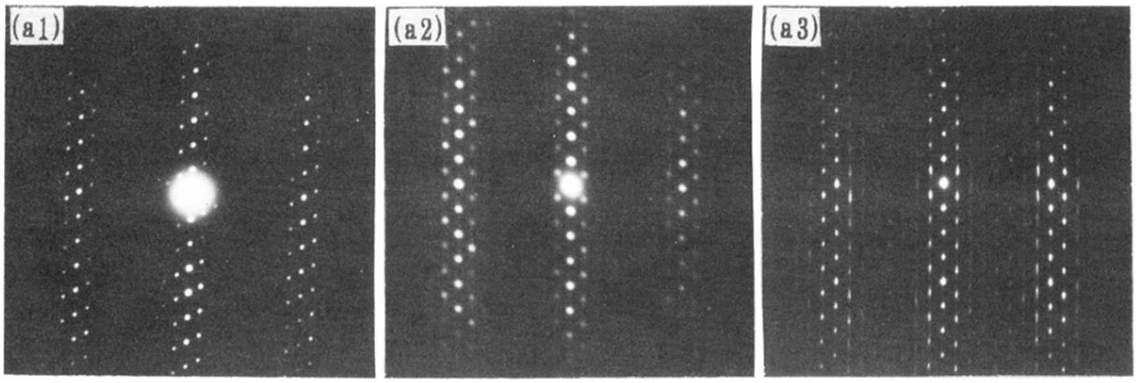

FIG. 6. The ED patterns along the [100]-zone axis of the samples $Bi_{2.1}Sr_{1.9-x}La_xCuO_y$; (a1) $x=0.2$; (a2) $x=0.6$; (a3) $x=1.0$.

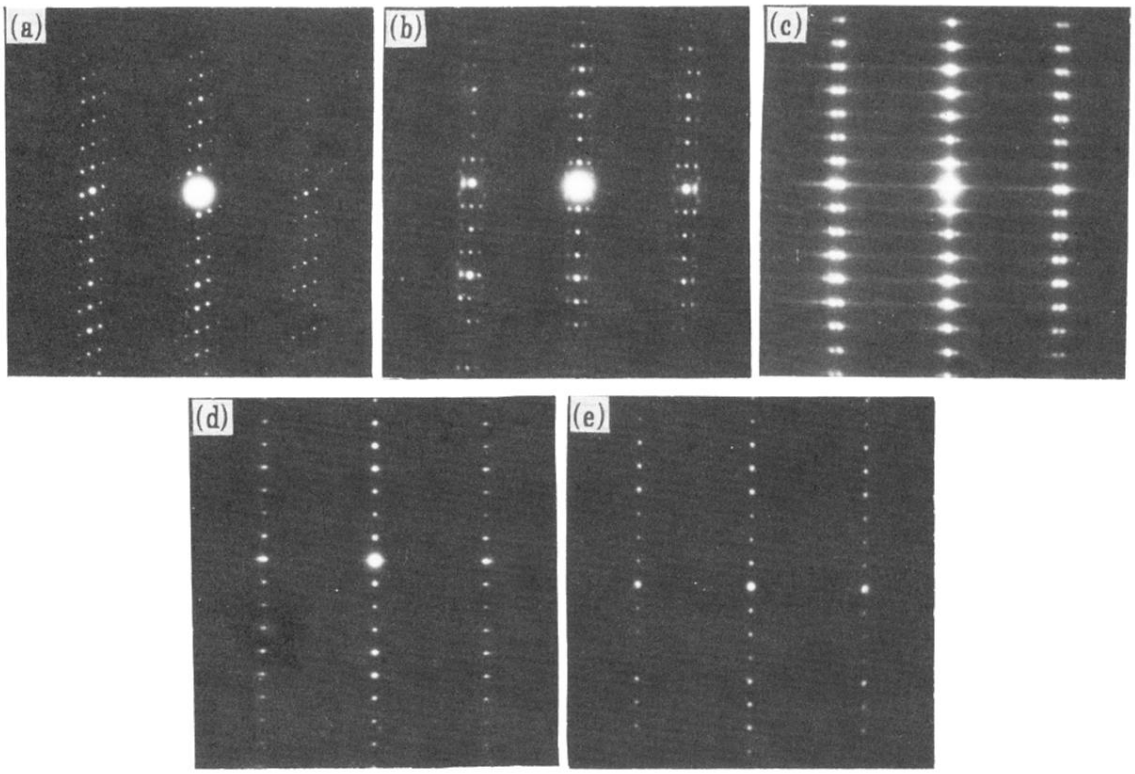

FIG. 7. The ED patterns along the [100]-zone axis of the samples $Bi_{2-x}Pb_xSr_2CuO_y$; (a) $x=0$; (b) $x=0.05$; (c) $x=0.2$; (d) $x=0.3$; (e) $x=0.6$.